Extracellular matrix and (re)myelination

Šišková, Zuzana

Chapter 3

Fibronectin impedes "myelin" sheet-directed flow in oligodendrocytes: a role for a beta 1 integrin-mediated PKC signaling pathway in vesicular trafficking

Zuzana Šišková, Wia Baron, Hans de Vries and Dick Hoekstra

Department of Membrane Cell Biology, Section Membrane Cell Biology, University Medical Center Groningen, University of Groningen, A. Deusinglaan 1, 9713 AV Groningen, The Netherlands

Molecular Cellular Neuroscience, 2006; in press

Abstract

Differentiation of oligodendrocytes results in the formation of the myelin sheath, a dramatic morphological alteration that accompanies cell specialisation. Here, we demonstrate that changes in the extracellular microenvironment may regulate these morphological changes by altering intracellular vesicular trafficking of myelin sheet-directed proteins. The data reveal that fibronectin, in contrast to laminin-2, decreased membrane directed transport of endogenous NCAM 140 and the model viral protein VSV G, both proteins normally residing in the myelin membrane. The underlying mechanism relies on an integrin-mediated activation of PKC, which causes stable phosphorylation of MARCKS. As a result, dynamic reorganization of the cortical actin cytoskeleton necessary for the targeting of vesicular trafficking to the myelin sheet is precluded, a prerequisite for morphological differentiation. These data are discussed in the context of the demyelinating disease multiple sclerosis, i.e., that leakage of fibronectin across the blood brain barrier may impede myelination by interference with intracellular myelin sheet-directed membrane transport.

Introduction

Cellular differentiation is often associated with morphological alterations, including changes in cell surface membrane structure and organization. Such changes may involve the formation of small membrane protrusions, such as the sprouting of microvilli, but also the biogenesis of extensive membrane structures, like myelin, which are formed upon differentiation of oligodendrocytes (OLGs) in the central nervous system. The formation of the myelin sheath and its wrapping around axons, necessary for mediating rapid and saltatory nerve impulse conduction, is an extreme example of cell specialisation, and depends on a dramatic increase in total cell surface area. Although myelin is still continuous with the oligodendroglial plasma membrane, both membrane domains display major differences in molecular composition (Podulso, 1981, Norton and Cammer, 1984, Deber and Reynolds, 1991). In fact, OLG may be regarded as polarized cells, like (polarized) epithelial and neuronal cells, with myelin sheaths as specialized subdomains of their plasma membranes (de Vries and Hoekstra, 2000, Kroepfl and Gardiner, 2001). Indeed, in parallel with apical and basolateral sorting in epithelial cells, our previous work (de Vries et al., 1998) revealed that vesicle-mediated delivery of myelin specific membrane proteins to the 'myelin' *sheet*, which is the *in vitro* equivalent of the non-compacted myelin *sheath in vivo*, shows typical properties of a basolateral-like trafficking mechanism whereas transport to the OLG plasma membrane shows features typical of an apical-like transport mechanism. During differentiation, myelin sheets are further locally 'polarized', presumably during compaction of the myelin membrane layers, as evidenced by the gradual acquirement of distinct molecular compositions of membrane subdomains within the sheet, thus adding to the potential complexity of traffic regulation in OLG (de Vries and Hoekstra, 2000, Kroepfl and Gardiner, 2001, Kramer et al., 2001).

However, little is known about how *de novo* myelin assembly and/or transport during maintenance are regulated. Previous work revealed that protein kinase C (PKC) activation inhibits morphological differentiation of OPCs (oligodendrocyte precursor cells) (Baron et al., 1999), implying that regulation of trafficking could involve activation or downregulation of PKC-mediated signaling pathways. Along such a mechanism, several extracellular cues might be envisioned as regulating factors in the onset of myelination. For example, fibroblast growth factor (FGF) completely blocks myelin sheet formation in OPCs, possibly via a PKC-dependent block in membrane traffic and inhibition of myelin gene expression (McKinnon et al., 1990, Asotra and Macklin, 1993, Baron et al., 2000). In contrast, the extracellular matrix (ECM) substrate, laminin-2, which is present on axons (Colognato et al., 2002), may promote myelin membrane formation, and its receptor, $\alpha 6\beta 1$ integrin, appears to be instrumental in this process, as both anti $\beta 1$ blocking antibodies and a dominant-negative approach inhibited laminin-

mediated myelination (Buttery and ffrench-Constant, 1999, Relvas et al., 2001). Interestingly, fibronectin, another ECM macromolecule, severely delays or even inhibits myelin sheet formation (Buttery and ffrench-Constant, 1999, Maier et al., 2005), suggesting a negative role of αv integrins, the only known fibronectin receptors present in OLGs. Intriguingly, fibronectin, absent in adult brain at normal conditions, enters the tissue upon disruption of the blood-brain-barrier at pathological conditions (Inoue et al., 1997), which occurs during multiple sclerosis, a demyelinating disease (Sobel and Mitchell, 1989).

Here, we have investigated whether ECM molecules such as laminin and fibronectin regulate intracellular vesicular traffic pathways of sheet-directed proteins in primary OLG cultures and an OLG-derived cell line, OLN 93. We show that fibronectin abrogates transport to the myelin sheet by activating an integrin β1-PKC-MARCKS-actin signaling pathway, thereby inhibiting morphological differentiation of OLGs and hence, myelination.

Materials and Methods

Materials

Dulbecco's Modified Eagle's Medium (DMEM), L-glutamine, penicillin/streptomycin were from GIBCO BRL (Life Technologies, Paisley, Scotland). Fetal calf serum (FCS) was obtained from Bodinco (Alkmaar, The Netherlands). PDGF-AA and FGF-2 were from Peprotech (Rocky Hill, NJ). Nonidet P40 (NP40) was purchased from Fluka BioChemica (Buchs, Zwitserland). Phorbol-12-myristate-13-acetate (PMA) and bisindolylmaleimide I (BIM) were obtained from Calbiochem-Novabiochem Corporation (La Jolla, CA). Paraformaldehyde (PFA) was supplied by Merck (Darmstadt, Germany). Sulfo-NHS-LC-Biotin was obtained from Pierce (Rockford, IL). Streptavidin–agarose was obtained from Upstate Lake Placid (New York, NY). Protease inhibitor cocktail tablets (Complete Mini) were obtained from Roche Diagnostics GmbH (Mannheim, Germany). All other chemicals were supplied by Sigma Chemical Co. (St. Louis, MO).

Antibodies

Polyclonal anti-rat-MARCKS antibody was a kind gift from Dr. Angus Nairn, New York, NY (Albert et al., 1986). Anti-VSV-G (IgG1) and anti-NCAM 140/180 (IgG2b) were purchased from Sigma Chemical Co. (St. Louis, MO). Anti-integrin β1 (CD29, Ha2/5, Hamster IgM) and anti-integrin β3 (CD61, F11, mouse IgG1) were supplied by BD Biosciences PharMingen. Anti-β5 integrin (P1F6, mouse IgG1) was purchased from Chemicon (Temecula, Ca). FITC- and TRITC-conjugated antibodies were obtained from Jackson ImmunoResearch Laboratories, Inc. (West Grove, PA). Secondary HRP-

conjugated antibodies were provided by Amersham Biosciences (Buckinghamshire, UK).

Cell culture

The oligodendroglia derived cell line OLN 93, a kind gift of Dr. Christiane Richter-Landsberg (Richter-Landsberg and Heinrich, 1996), were cultured in DMEM supplemented with 10% heat-inactivated FCS, L-glutamine, and the antibiotics penicillin and streptomycin (proliferation medium). Cells were trypsinized when they reached near-confluency and experiments were performed with passage 26-38. To test the effect of ECM components, the cells were cultivated on pre-coated poly-l-lysine (PLL, 5 μg/ml), laminin-2 (Ln2, 10 μg/ml) or fibronectin (Fn, 10 μg/ml) tissue culture flasks (Corning Incorporated Corning, NY). Flask were pre-coated for at least 3 hrs at 37ºC. For immunocytochemical studies cells were grown overnight on Lab-Tek chamber slides (Nalge Nunc) at a density of 10,000-15,000 cells per well. For the biochemical assays, cells were plated at a density of $1x10^6$ cells per dish and grown for 24 hrs. Cells used for PKC experiments were plated at a density of 500,000 cells/dish and grown on ECM coated dishes for 36 hrs or three days.

Primary oligodendrocyte culture

Primary mixed brain cell cultures were isolated from 1-3 day old Wistar rats as described previously (Baron et al., 2002). Briefly, rats were decapitated, forebrains were collected and by mechanical and enzymatic (papain) digestion a single cell suspension was obtained. Cells were cultured in DMEM, supplemented with 10% FCS, L-glutamine, penicillin and streptomycin for 10-14 days on PLL-coated tissue culture flasks (Nalge Nunc, Naperville, IL). OLG progenitors, growing on top of an astrocyte monolayer, were then isolated by a shake off procedure (McCarthy and de Vellis, 1980). After a 1hr pre-shake to remove contaminating microglia, flasks were shaken overnight at 240 rpm on an orbital shaker. The floating OLG progenitor cells obtained by this procedure were further purified via differential adhesion. Enriched OLG progenitors were synchronized in SATO medium (Maier et al., 2005), containing PDGF-AA (10 ng/ml) and FGF-2 (10 ng/ml) for 2 days. Differentiation was induced by growth factor withdrawal and cells were grown for 9 days (mature myelinating stage) in SATO medium supplemented with 0,5 % FCS with medium changes twice a week.

Immunocytochemical studies

Cells were first gently fixed with 2% paraformaldehyde (PFA) in phosphate buffered saline (PBS) for 15 min at room temperature (RT), followed by 4% PFA for 15 min at RT, after which they were permeabilized and blocked with 0.1% Triton X-100 and 10% FCS, respectively for 30 minutes at RT. Incubation with the primary antibody (MARCKS 1:100,

VSV G 1:50, NCAM 140/180 1:50) was then carried out for 30 min in the presence of 0.1% Triton X-100 and 2.5% FCS. This was followed by a wash and incubation for another 25 min with the appropriate fluorescently-conjugated secondary antibodies (FITC- and TRITC-conjugated antibodies 1:50-1:75). For actin filament staining, cells were fixed and permeabilized, and incubated for 30 min at RT with TRITC-labeled phalloidin (1 µg/ml). Nuclei were stained with DAPI. Mounting medium (1 mg/ml DABCO in 90% glycerol) was added to prevent image fading. The cells were analyzed with either a conventional fluorescence microscope (Olympus ProVis AX70) or a Leica TCS SP2 confocal system (Leica DMRXE microscope). Data were processed using Paint Shop Pro or Adobe Photoshop 7.0 software.

Western blot analysis

The cells were washed three times with PBS and harvested by scraping into PBS. Cells were centrifuged at 10.000 rpm at RT and pellets were lysed in TNE-lysis buffer (50mM Tris-HCL, 5mM EDTA, 150 mM NaCl, 1% Triton X-100 and protease inhibitor cocktail). Protein determination was performed by a Bio-Rad DC Protein Assay (Bio-Rad Laboratories, Hercules, CA), using BSA as a standard. Equal amounts of protein were mixed with 2x reducing SDS sample buffer, heated for 5 min at 98ºC and applied onto 10 % SDS-polyacrylamide gels. Proteins were transferred to a nitrocellulose membrane using a semi-dry blotting system for 1 hr (Bio-Rad, Hercules, CA) using a glycine-Tris-methanol buffer. The membranes were rinsed with Tris-buffered saline (TBS) and incubated for 1 hr at RT in blocking solution (5% nonfat dry milk in TBS). After washing, the membranes were incubated overnight with primary antibody (VSV G 1:1000, NCAM 140 1:250) in 1% nonfat dry milk in TBS containing 0.1% Tween 20 (incubation). The membranes were washed three times with TBS containing 0.1% Tween 20 (wash buffer) and incubated for 2 hrs with appropriate HRP-conjugated antibodies 1:2000) in incubation buffer and washed three times afterwards with wash buffer. Signals were detected by enhanced chemiluminescence (ECL; Amersham Pharmacia Biotech), scanned and processed using Paint Shop Pro and quantified with Scion Image software. To statistically analyze the data, PLL was set at 100% and Ln2 and Fn samples were determined as a percentage of this. Statistical analysis was performed using the appropriate Student's t-test. Values are expressed as means ± standard error of the mean (SEM). In all cases a p-value ≤ 0.05 was considered significant.

Viral infection

OLN 93 cells grown in proliferation medium were infected as described previously (de Vries et al., 1998). OLN 93 cells were infected when grown on non-coated tissue culture flasks, i.e. in the absence of any substrate for cell adhesion in order to prevent the effect of ECM substrates on the uptake of viral particles. Briefly, cells were infected for 1 hr at

37ºC with VSV virus (VSV strain San Juan A, a kind gift of Dr. Peter Rottier, Utrecht, The Netherlands) in serum-free culture medium, pH 6.8, without CO_2 . Then the virus was removed, fresh culture medium of pH 7.4 added, and the cells were incubated for an additional 1 hr at 37ºC and 5% CO_2 in the absence of FCS. After this, cells were trypsinized and plated on tissue culture dishes pre-coated with Fn, PLL and Ln2, and kept for 24 hrs at 37ºC and 5% CO_2 in serum-free medium. The PKC inhibitor BIM (0.5 µM), PKC activator PMA (200 nM) and the integrin functional blocking antibodies (10 µg/ml) were added immediately after cell trypsinization to the cell suspension and incubated for 30 min at 37ºC and 5% CO_2 in serum-free conditions, i.e. prior to plating on the different ECM substrates.

Primary OLG cultures were infected with VSV at the mature myelinating MBP stage as described above, except that SATO medium (pH 6.8) containing 0% serum was used for infection. After 1 hr, the SATO medium was refreshed, readjusted to standard pH, and, cells were incubated for 5-6 hrs at 37ºC and 5% CO_2 in the absence of serum.

PKC activation assay

A non-radioactive assay from Promega Corporation (Madison, WI) was used for detection of PKC activity. Briefly, cells were plated on the different substrates and the assay was carried out after approx 36 hrs or 3 days, according to the manufacturer's instructions. The cells were scraped in 1 ml of PBS, centrifuged at 7000 rpm, and the pellets were solubilized with TNE lysis buffer. Equal amounts of protein (60 µg) were loaded onto agarose gels and separated according to the electric charge of the fluorescent peptide, used as the PKC specific substrate that acquires the charge based on its phosphorylation. Gels were visualized under UV; pictures were scanned using Paint Shop Pro and quantified with Scion Image Software. To statistically analyze the data, PLL was set at 100% and Ln2 and Fn samples were determined as a percentage of this. A Student's t-test was applied for analysis. Values are expressed as means ± standard error of the mean (SEM). In all cases a p-value ≤ 0.05 was considered significant.

Surface biotinylation assay

Cells were washed twice with cold PBS and incubated with 0.1 mg/ml sulfo-NHS-LC-biotin for 25 min at 4ºC. Cells were washed three times for 2 min with cell wash buffer (65 mM Tris, 150 mM NaCl, 1mM $CaCl_2$, and 1mM $MgCl_2$, pH 7, 5) on ice, to remove excess biotin. Then cells were washed twice with PBS, scraped in 1 ml of PBS and centrifuged at 4ºC at 7000 rpm for 15 min. Protein concentrations were determined as described above. Equal amounts of proteins (50 µg) were adjusted to 250 µl with TNE-lysis buffer. To determine the intracellular/surface ratio, streptavidin–agarose (SA-agarose, 100 µl) was washed twice with 1ml IP wash buffer (cell wash buffer

supplemented with 0.35 M NaCl and 1% NP40). In between the wash steps, SA-agarose was centrifuged at 4ºC at 6000 rpm for 2 min. Samples were added to the washed SA-agarose and incubated overnight in a head over head tumbler at 4ºC. SA-agarose was separated from the non-bound supernatant fraction. The agarose (biotinylated proteins, i.e. surface localized) was washed four times with ice cold IP wash buffer, once with PBS, and boiled for 5 min at 100 ºC in 2x reducing sample buffer. Non-bound fractions (supernatant, non-biotinylated proteins, i.e. the fraction localized intracellularly) were concentrated by TCA precipitation. To each fraction 25 mg/ml of sodiumdeoxycholate was added, incubated for 5 minutes on ice, followed by precipitation with 6.5% trichloric acid (TCA) for 15 minutes on ice. Precipitates were centrifuged for 20 minutes at 13 000 rpm at 4ºC and the dry pellet was resuspended in 2x reducing SDS sample buffer. Samples from agarose and supernatant fractions were loaded onto SDS-PAGE gels and blotted as described above. To determine the expression of the integrin β subunits, the subunits were immunoprecipitated using protein-G sepharose similarly as described above for SA-agarose, followed by Western blotting and ECL detection, using HRP-conjugated SA.

Results

Fibronectin inhibits myelin sheet directed protein transport in primary oligodendrocytes

To determine whether ECM adhesive proteins could affect intracellular transport in OLGs, the flow of a viral protein, VSV G, previously shown to reflect myelin-directed transport (de Vries et al., 1998), was examined. Thus, primary OLG were cultivated on the ECM proteins laminin-2 (Ln2) or fibronectin (Fn), allowed to differentiate to the myelinating stage, and subsequently infected with VSV. Using the experimental protocol as described in Experimental Methods, the infection efficiency was nearly 100%, irrespective of the substrate on which the cells had been grown, and no significant differences in cell survival were observed (not shown; cf. de Vries et al., 1998). After 6 hrs, the intracellular distribution of VSV G was examined by immunofluorescence microscopy. In cells grown on Ln2, VSV G was distributed throughout the OLG cell body, and also localized to primary processes as well as the myelin sheet (fig.1A-C). This distribution is very similar as observed when the cells are grown on the inert substrate poly-l-lysine (PLL; not shown, cf. fig.1A-C), By contrast, in cells grown on Fn (fig. 1D-F), VSV G distribution was largely restricted to the cell body and only a very minor fraction reached the myelin sheet. Importantly, OLG differentiation *per se*, as defined by the expression of the myelin specific markers MBP and PLP, was not affected, nor did ECM substrates affect cell survival (not shown, cf. fig. 1). However, MBP-positive myelin sheets were less frequently observed (fig.1E), since in cells grown

on Fn, morphological differentiation, as assessed by myelin sheet formation, was usually dramatically retarded (Buttery and ffrench-Constant, 1999, Maier et al., 2005).

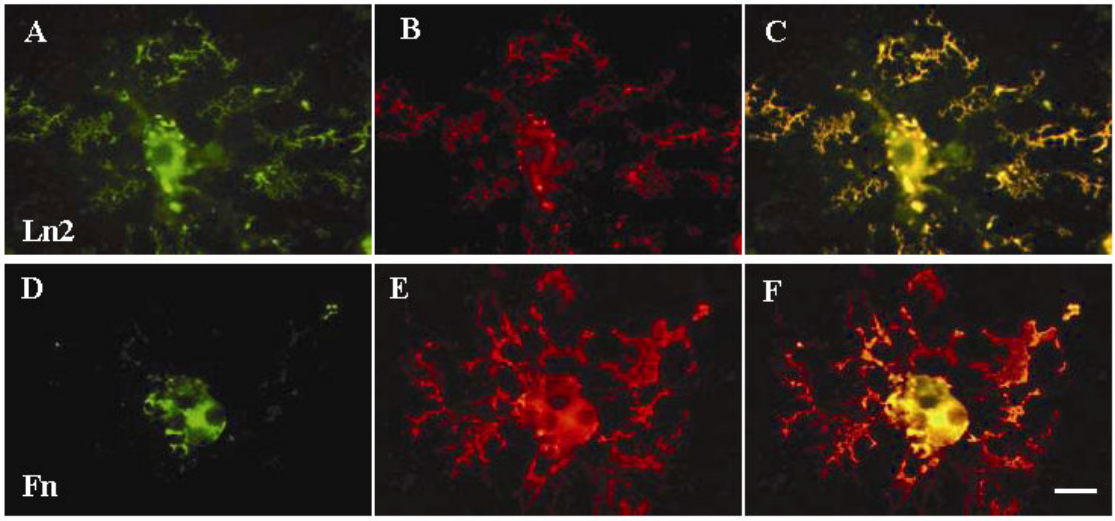

Figure 1. ***ECM-mediated effect on the transport of myelin sheet-directed protein VSV G in primary mature oligodendrocytes.*** *Primary mature oligodendrocytes in the MBP-stage were infected with VSV as described in Experimental Methods. After 6 hrs, the localization, i.e. cell surface or intracellular, of the viral protein VSV G was determined by immunofluorescence microscopy (A and D). In order to visualize myelin sheets, co-labeling with the major myelin specific protein MBP was performed (B and E). A-C) laminin-2; D-F) fibronectin. C) and F) merged pictures of VSV G and MBP using Adobe Photoshop software. At least 100 oligodendrocytes per well were analyzed in duplicate in three independent experiments of which representative pictures are shown. Scale Bar is 20 µm. Note that VSV G and MBP colocalize in myelin sheets when cells are grown on laminin-2, but not on fibronectin.*

In this context, it is relevant to emphasize that MBP is locally expressed in the sheet, following sheet-directed transport of its mRNA, which is presumably accomplished in a non-vesicular manner (de Vries et al., 1997). Since VSV G, being a transmembrane protein, is transported to the sheet by vesicule-mediated transport, exiting from the Golgi, the data thus imply that Fn in particular hampers the biogenesis of the myelin sheet, and/or its maturation, by impeding *de novo* membrane transport from body to sheet. To obtain further insight into the mechanism of this ECM-mediated impediment of membrane transport, the distinct transport steps following biosynthesis of sheet-specific macromolecules, were further investigated in an OLG-derived cell line OLN 93 which, under defined conditions, represents an established model for OPCs (Richter-Landsberg and Heinrich, 1996).

Fibronectin inhibits cell surface transport of myelin sheet directed proteins in OLN 93

A limited number of cells and difficulties in their biochemical handling and manipulation often frustrate research, using primary OLG cultures. Since pilot experiments revealed that blocking ECM-integrin interactions affected VSV uptake in OLG (data not shown),

while OLGs are difficult to remove from culture dishes, thus precluding viral infection prior to ECM exposure, we next examined whether the results obtained above could be reproduced in OLN 93 cells. OLN 93 is a cell line (Richter-Landsberg and Heinrich, 1996), derived from spontaneously transformed OLGs in primary rat brain glial cultures. In culture medium with high FCS levels (>5%), OLN 93 cells rapidly proliferate and resemble morphologically bipolar primary OPCs. At lower FCS levels (<1%), OLN 93 proliferate less and at lower cell densities acquire a morphology resembling newly-formed, premyelinating primary OLGs.

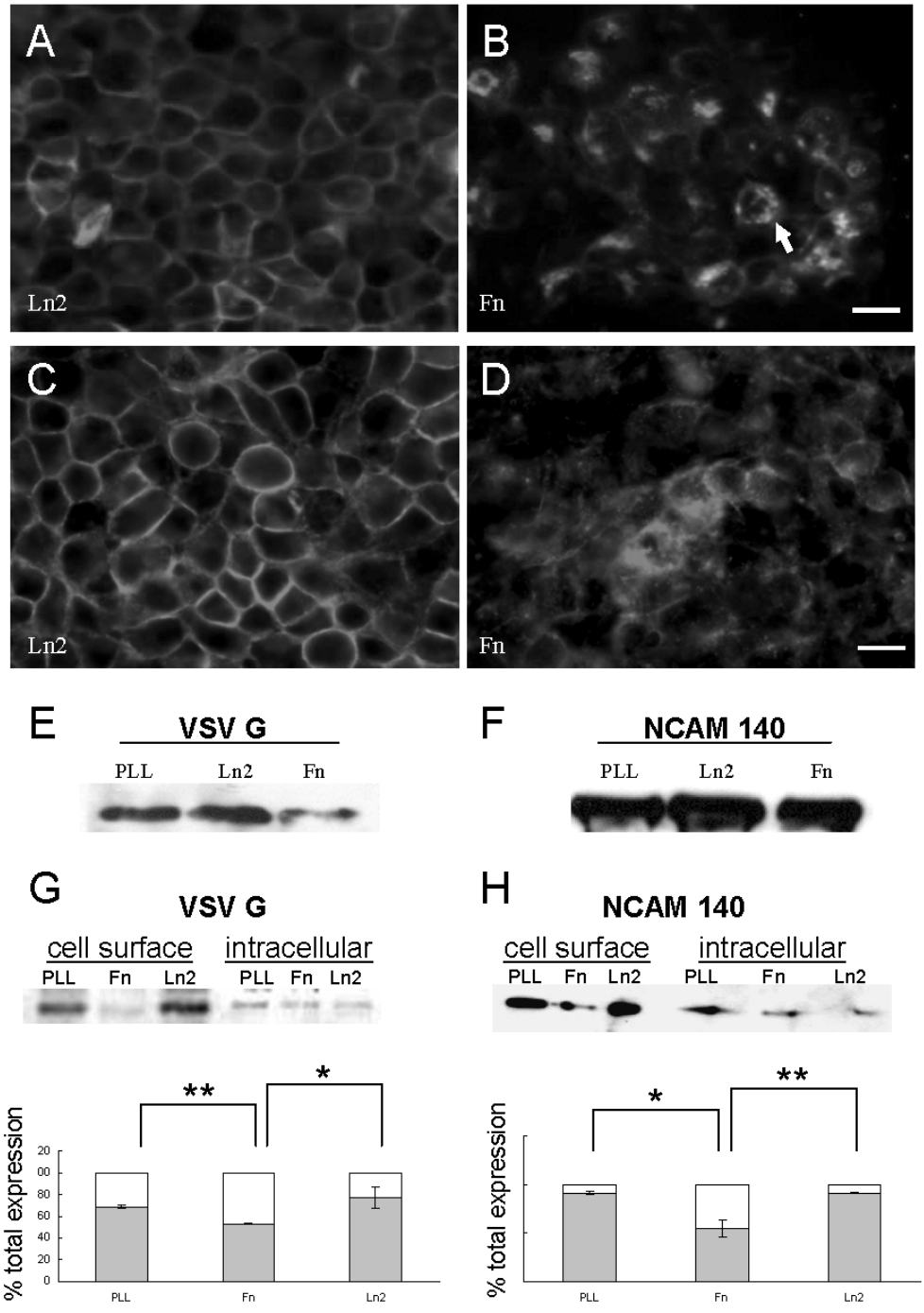

Figure 2. ***ECM-mediated effect on the transport of myelin sheet-directed proteins in OLN 93 cells.*** *Proliferating OLN 93 cells were infected with VSV on non-coated culture flasks as described in Experimental Methods, trypsinized and re-plated on PLL, fibronectin or laminin-2. After 24 hrs, the expression levels of the viral marker protein VSV G in total cell lysates were*

determined by Western blotting and the localization, i.e. at the cell surface or intracellularly, was determined by immunofluorescence microscopy and biochemically by making use of the ability to specifically label surface proteins with membrane impermeable biotin (see Experimental Methods). For visualization of endogenous NCAM 140, OLN 93 cells were treated and analyzed similarly, except for infection. A) VSV G localization on laminin-2, B) VSV G localization on fibronectin, C) NCAM 140 localization on laminin-2, D) NCAM 140 localization on fibronectin. In E) and F), the overall expression levels of VSV G and NCAM 140, respectively, are shown in cells grown on different substrates, as indicated. In G) and H), the fractional distribution of VSV G and NCAM 140, respectively, present at the cell surface (lower, grey bar) and intracellularly (upper, white bar), is shown, as determined by biotinylation and immunoprecipitation (for details, see Experimental Methods). The data are expressed as a fraction of the total expression (set at 100%). Data represent means of at least three independent experiments ± SEM ($p<0.05$, and ** $p<0.01$). Representative pictures and blots of at least three independent experiments are shown. Note that in cells grown on fibronectin the fraction of VSV G (fig. 2B, arrow and fig. 2G) and NCAM 140 (fig. 2D and fig. 2H) associated with the plasma membrane was significantly decreased, as compared to the fractional distribution of VSV G in cells, grown on laminin-2 and PLL.*

To exclude an ECM-dependent interference with the efficiency of VSV infection, proliferating OLN 93 cells, growing on non-coated culture flasks, were infected with the virus. The cells were subsequently trypsinized and further cultured on the desired ECM substrate, as described in Experimental Methods. After 24 hrs, the intracellular distribution of VSV G was examined by immunofluorescence microscopy. It should be noted that at these experimental conditions, i.e., when cells were plated at a relatively high density, and at only 1 day after the onset of differentiation, OLN 93 cells do not acquire a complex morphology. Yet, as shown in figure 2A, in cells grown on Ln2, VSV G predominantly localizes to the plasma membrane, as reflected by bright rings marking the plasma membrane boundary, whereas on Fn a large proportion of the protein accumulates intracellularly (fig. 2B, arrow). A similar plasma membrane-localized appearance was seen when the cells were grown on (inert) PLL (data not shown). Hence, as observed for ECM dependent transport in primary cultures of OLGs, when cells were grown on Fn, but not Ln2, membrane directed transport, i.e., to plasma membrane and/or myelin sheet, is impeded.

To obtain further support for a genuine localization of VSV G in the plasma membrane of the OLN 93 cells, a quantitative biochemical analysis, relying on biotinylation of cell surface localized VSV G, was carried out. As shown in Figure 2G at least 70-80% of the total pool of VSV G was present at the surface of cells grown on either PLL or Ln2, whereas approximately 40-50 % of the protein reached the surface in cells grown on Fn. Interestingly, the distribution of the major fraction of VSV G corresponded to the localisation of the trans-Golgi marker APA-1, suggesting that the observed frustration in plasma membrane directed transport may at least in part rely on a delay in exit from the Golgi (data not shown). It should also be noted that the overall expression of VSV G was decreased by approx. 50% in cells grown on Fn, as compared to that obtained for Ln2 (fig. 2E). This difference in expression level is due to interference of the Fn matrix with VSV G synthesis, and not to differences in viral entry, as OLN 93 cells were exposed to Fn *after* VSV infection.

To corroborate these data for endogenous proteins, we next investigated the effect of the ECM on the cell surface expression of NCAM 140, typically present in the myelin sheath in OLGs (Massaro, 2002). As shown in fig. 2H, in OLN 93 cells grown on Fn, the cell surface appearance of NCAM 140 is substantially reduced, indicating that transport of an intrinsically expressed myelin-directed protein is also regulated by the ECM. Similarly as observed for myelin protein expression in primary OLG, no significant differences in NCAM 140 expression levels were observed in OLN 93 cells grown on either Fn or Ln2 (fig. 2F). On all substrates, the NCAM 180 isoform was not detectable in OLN 93 cells. As observed for VSV G, NCAM 140 is primarily localized to the plasma membrane in cells grown on Ln2 (fig. 2C), whereas on Fn (fig. 2D) NCAM 140 is localized intracellularly. Taken together, these results imply that distinct ECM compounds are able to modulated intracellular traffic pathways in OLN 93 cells, similarly as observed for myelin sheet directed transport in primary OLGs. We therefore considered OLN 93 cells to represent an appropriate cell model to further clarify the ECM-dependent regulation of surface transport of myelin-sheet directed proteins. In fact, it was also noted that when OLN 93 cells were plated at a low density, Ln2 promoted cell spreading, which might be suggestive of attempts to make myelin-sheet like structures (unpublished observations). Next, we examined in OLN 93 whether integrins, the main receptors by which cells bind and respond to ECM molecules, were involved as intermediates in regulating ECM-dependent trafficking.

Inhibition of plasma membrane directed transport on fibronectin is mediated by β1 integrin

αv integrins i.e. integrin αvβ1, αvβ3, αvβ5 and αvβ8, have been identified as Fn receptors on the surface of OLGs (Milner and ffrench-Constant, 1994, Milner et al., 1997), whereas the traditional Fn receptors, such as integrin α4β1, α5β1and α8β1 are not detectable on cells of the OLG lineage (Milner and ffrench-Constant, 1994). In figure 3D it is shown that OLN 93 cells expressed the αv integrins, integrin αvβ1, αvβ3, and αvβ5, as determined by surface biotinylation. To determine, therefore, whether integrin ligation might be responsible for the impeded intracellular membrane flow on fibronectin, we next examined whether function-perturbing antibodies against the integrin subunits β1, β3, and β5 could restore plasma membrane directed transport in OLN 93 cells. To our knowledge, appropriate functional blocking antibodies against rat β8 subunits are not available, which are therefore not included in this study. Interestingly, as opposed to a prominent intracellular localization of VSV G in cells grown on Fn per se (cf fig. 2A), a predominant plasma membrane localization was apparent when the cells had been cultured on the same ECM substrate, but in the presence of β1 integrin functional blocking antibody (fig. 3A). In contrast, functional blocking antibodies against β3 and β5 integrin were unable to relieve the traffic block, and major fractions of VSV G were still

largely localized in intracellular compartments (fig. 3B and 3C, respectively). Importantly, these effects were strictly related to adhesion of the cells to the Fn substrate, since VSV G localization in cells grown on Ln2 was not altered by any of these compounds (data not shown). Furthermore, the steady-state surface expression of αv integrins as determined by surface biotinylation, was not affected by Fn, thus serving as a useful control, suggesting that not all membrane proteins are repressed by Fn and, moreover, that integrins follow a different traffic pathway to the membrane than myelin-sheet directed proteins. Taken together, these data suggest that a β1 integrin is transducing the Fn signal across the membrane thereby preventing surface directed vesicular transport of myelin-sheet directed proteins.

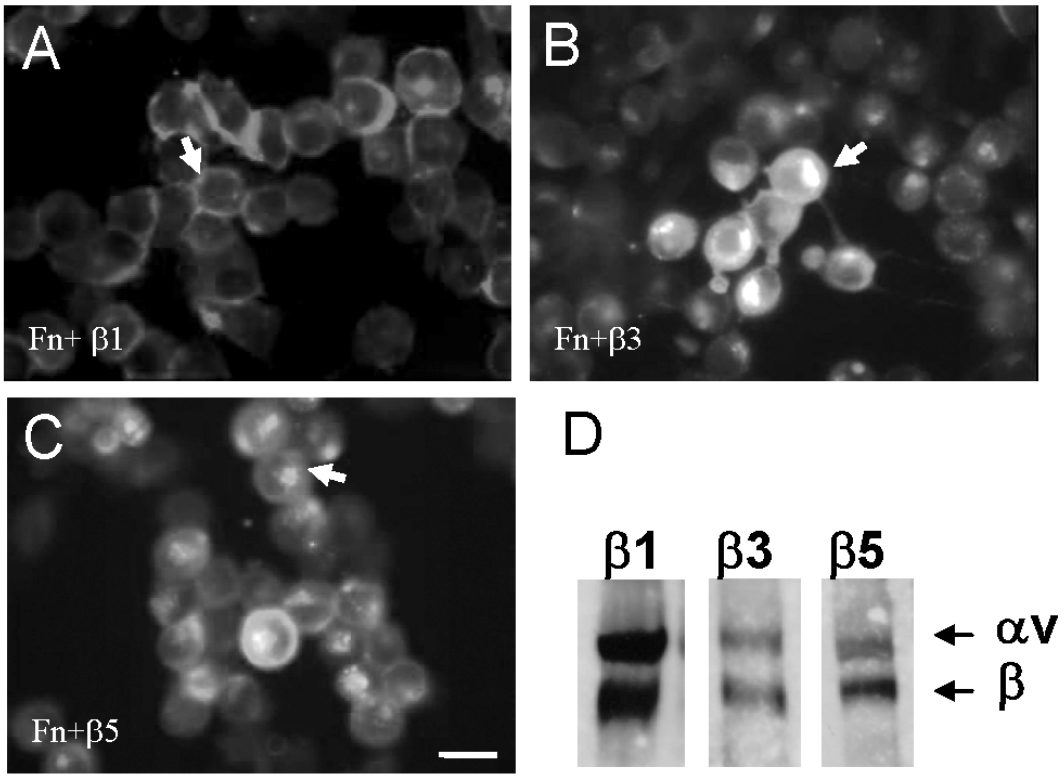

Figure 3. ***Effect of functional integrin blocking antibodies on VSV G trafficking on fibronectin.*** *Proliferating OLN 93 cells grown on non-coated dishes were infected with VSV, trypsinized, and subsequently cultured on fibronectin in the continuous presence of functional integrin blocking antibodies (β1, β3, and β5) as described in Experimental Methods. After 24 hrs VSV G localization was determined by immunofluorescence microscopy. A) β1, B) β3, and C) β5. Representative pictures of three independent experiments are shown. Scale bar is 20μm. Note that β1 perturbing antibodies were able to reverse the block in cell surface transport on fibronectin (fig.3A cf fig.2B), whereas in the presence of β3 and β5 functional antibodies transport is still inhibited (fig. 3B and 3C cf fig. 2B). D) Cell surface expression of integrin β1, β3, and β5 subunits in proliferating OLN 93 cells (non-coated dishes) as determined biochemically by surface biotinylation and immunoprecipitation. Representative blots of at least three independent experiments are shown.*

In previous work, studying the regulation of intracellular trafficking in relation to OLG differentiation, we identified PKC as a potent negative regulator in plasma membrane

directed transport in OLGs (Baron et al., 1999). Therefore, we next examined whether PKC activation might act as the intracellular signal target of the Fn-integrin interaction in OLN 93 cells.

PCK activity is involved in fibronectin-mediated impediment of cell surface protein transport

In both OPCs (Baron et al., 1999) and mature OLGs (unpublished observations), PKC activation impedes cell surface integration of VSV G by inhibiting docking of VSV G-containing transport vesicles to the plasma membrane.

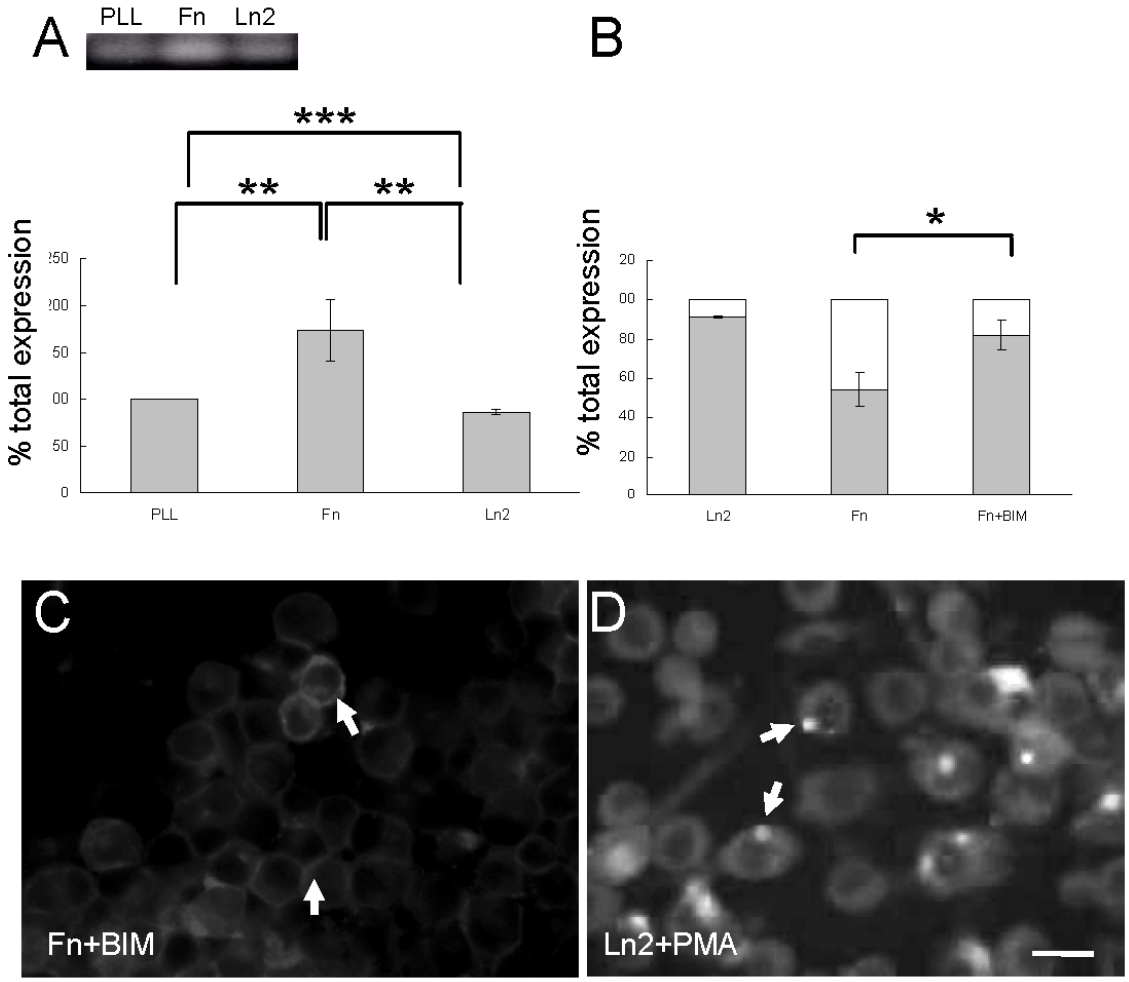

Figure 4. ***Role of PKC in modulation of intracellular trafficking routes by ECM in OLN 93 cells.*** *A) ECM-mediated effects on PKC activity were determined by a non-radioactive PKC assay as described in Experimental Methods. As illustrated in a representative picture, cells grown on fibronectin showed an increased PKC activity. The PKC activity was quantified, and bars represent means of five independent experiments ± SEM, * p<0.05, ** p<0.01, and *** p<0.001. PKC activation on PLL has been set to 100%. B) Cell surface and intracellular distribution of NCAM 140 in OLN 93 cells were determined by surface biotinylation. Cell surface fraction (lower grey bar) and intracellular fraction (upper white bar) of total expression (set at 100%) are shown. Bars represent means of three independent experiments * p<0.05, ** p<0.01, and *** p<0.001. Note that the cell surface fraction of NCAM 140 on fibronectin is significantly higher after BIM treatment as compared to control. C) and D) proliferating OLN 93 cells were infected, trypsinized and cultured on fibronectin in the presence of BIM (C), or on laminin-2 in the presence of the PKC activator, PMA (D). Appearance of VSV G protein 24 hrs after infection is shown, representative of three independent experiments. Scale bar is 20 µm. Note that the plasma membrane fraction of VSV G substantially increased, when cells cultivated on fibronectin*

were incubated in the presence of the PKC inhibitor BIM (C, arrows). In contrast, PKC activation on laminin-2 resulted in intracellular accumulation (D, arrows).

We therefore determined whether the level of PKC activity was affected in OLN 93 cells, when grown on different ECM. Remarkably, as shown in figure 4A, in cells grown on Fn, PKC activity was significantly increased compared to cells grown on either PLL or Ln2. To establish whether the enhanced PKC activity in cells grown on Fn was instrumental in frustrating intracellular protein traffic, we next determined whether PKC inhibition could counteract the block in cell surface-directed protein transport. Quantitative biochemical analysis of cell surface localized protein fractions of NCAM 140 by means of biotinylation and immunoprecipitation (see Experimental Methods) revealed that the PKC inhibitor BIM indeed counteracted the inhibitory effect of Fn on cell surface transport. Thus, in the presence of BIM the fraction of NCAM 140 that reached the cell surface in cells grown on Fn was similar to that in cells grown on Ln2 (fig. 4B). Consistent with these data were immunofluorescence microscopy observations, showing that in the presence of BIM, the cells typically display a ring of fluorescence marking the plasma membrane boundary of the cells, very reminiscent as observed for cells grown on Ln2 (fig. 4C compare to fig. 2A, arrows). As a control, PKC inhibition by BIM did not significantly affect the plasma membrane appearance of VSV G when cells were cultured on Ln2 or PLL (data not shown). In contrast, upon PMA (200 nM)-induced activation of PKC, protein transport to the plasma membrane of OLN 93 cells, grown on Ln2, was effectively impeded, very similar as observed in cells grown on Fn (fig. 4D, compare to fig. 2B, arrows). Taken together, these data underscore the importance of PKC in regulating intracellular trafficking routes.

MARCKS phosphorylation on fibronectin prevents dynamic actin cytoskeleton remodelling

To further assess the underlying mechanism downstream of the Fn-mediated activation of PKC, we next examined the cellular distribution of a major PKC substrate in OLGs, MARCKS. Previous work has shown that activation of PKC induced the predominant phosphorylation of MARCKS, which in turn regulates the structuring of the actin cytoskeleton, both in OPCs (Baron et al., 1999, Baron et al., 2000) and myelinating OLGs (Baron, unpublished observations). As shown in figure 5A, in OLN 93 cells cultured for 36 hrs on Ln2 or PLL (not shown), MARCKS is largely plasma membrane associated. By contrast, in cells grown for 36 hrs on Fn (fig. 5B), a considerable fraction of the protein was detected in the cytoplasm.

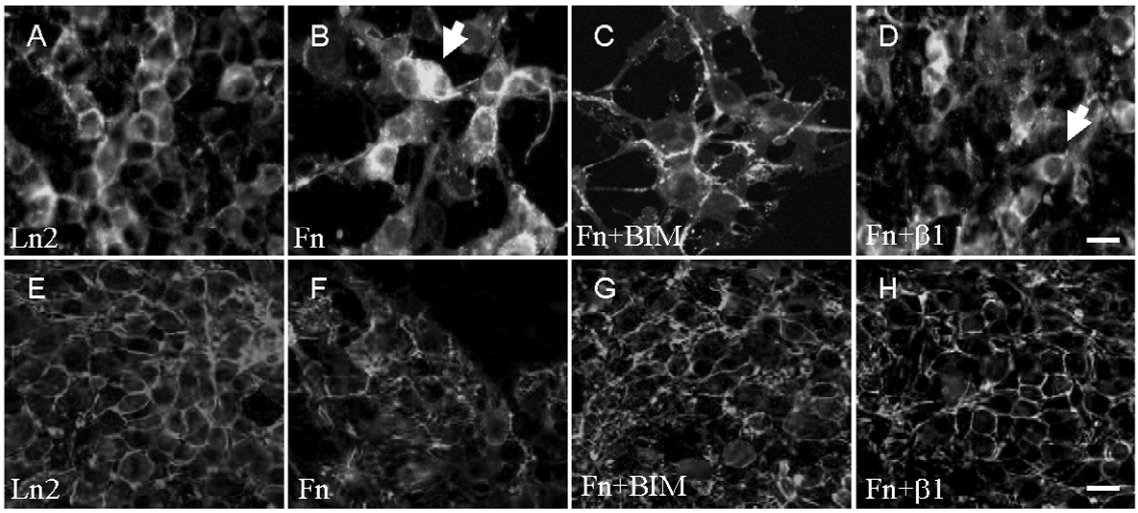

Figure 5. ***ECM-mediated effect on MARCKS and cytoskeleton distribution in OLN 93 cells.*** *A) – D) and I) Cellular distribution of MARCKS in proliferating OLN 93 24 hrs after trypsinization was determined by immunofluorescence microscopy. A) laminin-2, B) fibronectin, C) fibronectin and BIM, D) fibronectin and β1 functional blocking antibody. Representative pictures of three independent experiments are shown. Scale bar is 20 µm. Note that cells grown on fibronectin show a predominant MARCKS localization in the cytosol, in contrast to laminin-2. PKC inhibitor BIM and β1 blocking antibody treatment counteracted the cytosolic localization. E)-H) Actin appearance of proliferating OLN 93 cells 24 hrs after trypsinization is visualized by TRITC-labeled phalloidin and confocal microscopy. E) laminin-2, F) fibronectin, G) fibronectin and BIM and H) fibronectin and β1 functional blocking antibody. Representative pictures of three independent experiments are shown. Scale bar is 20 µm. Note, that on fibronectin the continuous line of cortical actin is perturbed as compared to the actin distribution in cells grown on laminin-2, an effect which was counteracted by BIM and β1 functional blocking antibody.*

This cytosolic localization of MARCKS appeared to be permanent, as even after 3 days MARCKS still largely localized to the cytosol of cells, grown on Fn (data not shown). This distribution of MARCKS is entirely consistent with the PKC activity data, taking into account that upon phosphorylation MARCKS translocates from the plasma membrane to the cytosol. Indeed, following treatment of the cells grown on Fn with the PKC inhibitor BIM, a considerable fraction of MARCKS was no longer present in the cytosol and reallocated to the plasma membrane (fig. 5C). Similarly, in the presence of β1 integrin blocking antibody, MARCKS was predominantly plasma membrane localized (fig. 5D), indicating that MARCKS translocation is mediated by PKC activation, downstream of β1 integrin signaling. Integrin β3 and β5 function-perturbing antibodies were not able to counteract the permanent translocation of MARCKS in cells grown on Fn, thus emphasizing β1 integrin specificity (data not shown).

Since dephosphorylated MARCKS is an actin filament cross-linking protein that is particularly involved in the interaction between actin cytoskeleton and plasma membrane, the organization of actin filaments in OLN 93 cells, grown on the different ECM, was examined next. In OLN 93 cells cultured on Ln2 (fig. 5E) or PLL (not shown), the actin cytoskeleton, as visualized by confocal microscopy after staining with TRITC-labeled phalloidin, is apparent as a sharp, continuous aligning on the edges of the

plasma membrane. The apparent continuity of this pattern of cortical actin distribution appears to be perturbed in cells grown on Fn (fig 5F), and the actin cytoskeleton is partly redistributed to the cytosol. As for MARCKS translocation, this perturbation of cortical actin cytoskeleton distribution is persistent, as after 3 days in culture similar results were obtained (data not shown). However, in the presence of BIM (fig. 5G) and even more pronounced in the presence of β1 integrin blocking antibody (fig. 5H), actin filaments became aligned again with the plasma membrane in cells grown on Fn, and their appearance is similar as observed in cells grown on Ln2 (fig. 5E). Inhibition of PKC activity had no effect on cortical actin distribution when cells were grown on Ln2 or PLL (data not shown). Hence, on Fn, permanently phosphorylated MARCKS, downstream of β1 integrin-mediated PKC activation, is unable to properly orient actin filament distribution.

Discussion

The present work has provided novel insight into mechanisms by which ECM proteins regulate myelin sheet development in OLGs. Thus, the data reveal that in contrast to Ln2, Fn impeded biosynthetic protein trafficking to the myelin sheet, and that the underlying mechanism is most likely related to a β1 integrin mediated activation of PKC. As a result, the major PKC substrate, MARCKS, becomes permanently phosphorylated, causing its translocation into the cytosol, which in turn will lead to an inhibition of dynamic actin cytoskeleton remodelling. The data imply that these events, which occur just underneath the cell body plasma membrane, are apparently highly relevant for myelin sheet-directed protein transport, since in cells grown on Fn, myelin sheet biogenesis is aberrant or is at least strongly delayed (Buttery and ffrench-Constant, 1999, Maier et al., 2005). This is reflected by the impediment of MBP integration and transport of myelin sheet proteins, including the marker protein VSV G and endogenous NCAM 140, rather than an effect on the *de novo* biosynthesis of myelin specific proteins, which thus causes their accumulation within the cell body. Since Fn may gain access into sclerotic lesions during inflammation at pathophysiological conditions (Sobel and Mitchell, 1989), the present work also bears relevance to developments seen in the demyelinating disease multiple sclerosis, where myelin is degraded and remyelination of axons precluded. It is of interest in this context that Ln2, which associates with axons at regular physiological conditions (Colognato et al., 2002), enhances myelin membrane formation by permitting myelin sheet directed transport, which correlates well with strongly reduced PKC activity levels.

PKC is known to be involved in OLG differentiation and myelination at various levels, including the regulation of proliferation, differentiation, myelin sheet formation, and myelin protein gene expression (Avossa and Pfeiffer, 1993, Asotra and Macklin, 1993,

Baron et al., 1998, Baron et al., 2002). In particular, pharmacological activation of PKC suppresses myelin protein expression (Asotra and Macklin, 1993) and plasma membrane insertion of newly synthesized proteins (Baron et al., 1998, this study). Evidently, Fn-mediated PKC activation did not suppress the expression of myelin proteins, as both the amount of MBP expressing cells and levels of the myelin specific proteins MBP and PLP were very similar in cells grown on either Fn or Ln2 (Buttery and ffrench-Constant, 1999, Maier et al., 2005, and our unpublished observations). This would suggest that perturbation of transport and downregulation of myelin protein synthesis are not causally related. In addition, it is possible that pharmacological activation leads to a higher PKC activity than Fn-activation, which would thus imply that regulation of transport is more sensitive to PKC activity than protein expression.

The increased PKC activity on Fn that perturbs cell surface directed transport, is likely due to ligation of a β1 integrin. In contrast to β3 and β5 blocking antibodies, a β1 integrin functional blocking antibody was able to counteract the Fn-mediated block in myelin sheet protein directed transport. There is mounting evidence that PKC is also able to regulate the expression and distribution of integrins themselves. In fact, different PKC isoforms have been shown to regulate the cellular distribution of β1 integrin, actively contributing to cell motility (Ivaksa et al., 2005, Ng et al., 1999). However, in OLGs, surface levels of αv integrins are not affected by Fn, and PKC-integrin interactions have been shown to be very important for OLGs development and behaviour. For example, physiological concentrations of PDGF stimulate a PKC dependent activation of integrin αvβ3, which in turn induces OLG proliferation (Baron et al., 2002). Here, we report the reverse process to occur, i.e., integrin control over PKC activity. Thus, Fn-mediated activation of PKC downstream of integrin β1 perturbs myelin sheet directed traffic. Whether β1 integrin activates PKC directly or via intermediate signal transducers, such as PI-PLC and PI3K, remains to be determined. In summary, in OLGs, bi-directional PKC-integrin linkages appear to exist, involving different integrin heterodimers and probably different PKC isoforms (Asotra and Macklin, 1994). Thus, a PKC-mediated control over integrin αvβ3 and α6β1 activity (Baron et al., 2002, Decker and ffrench-Constant, 2004, Baron et al., 2005) and β1 integrin-mediated control over PKC activity can be discerned.

Our data further suggest that Fn-activated PKC causes a permanent displacement of MARCKS, due to its phosphorylation, into the cytosol, thereby eliminating its concomitant interaction with plasma membrane and cytoskeleton. This results in a 'frozen' actin cytoskeleton that interferes with vesicular trafficking towards the myelin sheet. The persistent cytosolic localization of MARCKS on Fn might be related to the fact that PKC activity is difficult to downregulate in OLGs (Yong et al., 1991, Asotra and Macklin, 1994, Baron et al., 1998) and in OLN 93 cells (our unpublished observations). Interestingly, dynamic MARCKS phosphorylation has been shown to be a key event in

regulating morphological changes during initial adhesion and subsequent cell spreading (Disatnik et al., 2004), the latter requiring inactivation of PKC, and reallocation of MARCKS to the plasma membrane. As extension of myelin sheets entails continuous cell spreading requiring membrane-associated MARCKS, the persistent cytosolic localization of MARCKS on Fn could explain the perturbation of myelin biogenesis.

The present system may also serve as a convenient but simplified model to understand as to how pathophysiological changes in the ECM microenvironment may influence OLG differentiation, and hence myelination. Disruption of the blood brain barrier, as occurs during multiple sclerosis, facilitates the deposition of Fn (Sobel and Mitchell, 1989), raising the issue to what extent this and other matrix proteins may interfere with remyelination events. The current study strongly supports the possibility that leakage of Fn across the blood brain barrier indeed may influence myelin formation of the OPCs present within MS lesions by interference with fundamental cellular events like polarized membrane directed transport.

In conclusion, this study demonstrates a connection between ECM-dependent adhesion and (polarized) vesicular trafficking, necessary for the biogenesis of myelin. Such a coupling seems also necessary for cell motility, since the myelin marker protein VSV G is selectively transported to the leading edge of a migrating cell (Bergmann et al., 1983, Kupfer et al., 1987). Also from a therapeutic point of view, integrin-mediated control of myelination is worth considering. For example, *in vivo*, myelin membrane formation appears to be initiated upon contact of the tips of OLG processes with axonal Ln2. In line with the present work, these observations emphasize the potential role of ECM in triggering localized membrane polarity development, involving exclusive myelin-specific targeting to an OLG process in contact with an axon.

Acknowledgments

Z.S. is a recipient of a PhD fellowship from the Graduate School of Behavioral and Cognitive Neurosciences, University of Groningen, The Netherlands. This work was supported by grants from the Dutch Foundation for the Support of MS Research 'Stichting MS Research' to W.B. (01-438 MS), and the Foundation 'Jan Kornelis de Cock'. We thank all members of the Hoekstra lab for inspiring discussions.

References

Albert, K.A., Walaas, S.I., Wang, J.K.-T., Greengard, P., 1986. Widespread occurrence of '87 kDa', a major specific substrate for protein kinase C. Proc. Natl. Acad. Sci. USA 83, 2822-2826.

Asotra, K., Macklin, W.B., 1993. Protein kinase C activity modulates myelin gene expression in enriched oligodendrocytes. J. Neurosci. Res. 34, 571-588.

Asotra, K., Macklin, W.B., 1994. Developmental expression of protein kinase C isozymes in oligodendrocytes and their differential modulation by 4 beta-phorbol-12,13-dibutyrate. J. Neurosci. Res. 39, 273-89.

Avossa. D., Pfeiffer, S.E., 1993. Transient reversion of O4+GalC- oligodendrocyte progenitor development in response to phorbol ester TPA. J. Neurosci. Res. 34, 113-128.

Baron, W., de Vries, E.J., de Vries, H., Hoekstra, D., 1999. Protein kinase C prevents oligodendrocyte differentiation: modulation of actin cytoskeleton and cognate polarized membrane traffic. J. Neurobiol. 41, 385-98.

Baron., W., Metz, B., Bansal, R., Hoeksta, D., de Vries, H., 2000. PDGF and FGF-2 signaling in oligodendrocyte progenitor cells: regulation of proliferation and differentiation by multiple intracellular signaling pathways. Mol. Cell. Neurosci. 15, 314-329.

Baron, W., Shattil, S.J., ffrench-Constant, C., 2002. The oligodendrocyte precursor mitogen PDGF stimulates proliferation by activation of alpha(v)beta3 integrins. EMBO J. 21, 1957-1966.

Baron, W., Colognato, H., ffrench-Constant, C., 2005. Integrin-growth factor interactions as regulators of oligodendroglial development and function. Glia 49, 467-479.

Bergmann, J.E., Kupfer, A., Singer, S.J., 1983. Membrane insertion at the leading edge of motile fibroblasts. Proc. Natl. Acad. Sci. USA 80, 1367-1371.

Buttery, P.C., ffrench-Constant, C., 1999. Laminin-2/integrin interaction enhance myelin membrane formation by oligodendrocytes. Mol. Cell Neurosci. 14, 199-212.

Colognato, H., Baron, W., Avellana-Adalid, V., Relvas, J. B., Baron-Van Evercooren, A., Georges-Labouesse, E., ffrench-Constant, C., 2002. CNS integrins switch growth factor signaling to promote target-dependent survival. Nat. Cell Biol. 4, 833-841.

Decker, L., ffrench-Constant, C., 2004. Lipid rafts and integrin activation regulate oligodendrocyte survival. J. Neurosci. 24, 3816-3825.

Deber, C.M., Reynolds, S.J., 1991. Central nervous system myelin: structure, function and pathology. Clin. Biochem. 24, 113-134.

de Vries., H., de Jonge, J.C., Schrage, C., van der Haar, M.E., Hoekstra, D., 1997. Differential and cell developmental-dependent localization of myelin mRNAs in oligodendrocytes. J. Neurosci. Res. 47, 479-488.

de Vries, H., Schrage, C., Hoekstra D., 1998. An apical-type trafficking pathway is present in cultured oligodendrocytes but the sphingolipid-enriched myelin membrane is the target of a basolateral-type pathway. Mol. Biol. Cell. 9, 599-609.

de Vries, H., Hoekstra, D. 2000. On the biogenesis of the myelin sheath: cognate polarized trafficking pathways in oligodendrocytes. Glycoconj. J. 17, 181-190.

Disatnik M. H., Boutet, S.C., Pacio, W., Chan, A.Y., Ross, L.B., Lee, C.H., Rando T. A., 2004. The bi-directional translocation of MARCKS between membrane and cytosol regulates integrin-mediated muscle cell spreading. J. Cell Sci. 117, 4469-4479.

Inoue, A., Koh, C.S., Yamazaki, M., Yanagisawa, N., Ishihara, Y., Kim, B.S., 1997. Fibrin deposition in the central nervous system correlates with the degree of Theiler's murine encephalomyelitis virus-induced demyelinating disease. J. Neuroimmunol. 77., 185-194.

Ivaska, J., Vuoriluoto, K., Huovinen, T., Izawa, I., Inagaki, M., Parker, P.J., 2005. PKCepsilon-mediated phosphorylation of vimentin controls integrin recycling and motility. EMBO J. 24, 3834-3845.

Kupfer, A., Kronebusch, P.J., Rose, J.K., Singer, S.J., 1987. A crictical role for the polarization of membrane recycling in cell motility. Cell. Motil. Cytoskeleton 8, 182-189.

Kramer, E.M., Schardt, A., Nave, K.A., 2001. Membrane traffic in myelinating oligodendrocytes. Microsc. Res. Tech. 15, 656-671.

Kroepfl, J.F., Gardinier, M.V., 2001. Mutually exlcusive apicobasolateral sorting of two oligodendroglial membrane proteins, proteolipid protein and myelin/oligodendrocyte glycoprotein. J. Neurosci. Res. 15, 1140-1148.

Maier, O., van der Heide, T., van Dam, A.M., Baron, W., de Vries, H., Hoekstra, D., 2005. Alteration of the extracellular matrix interferes with raft association of neurofascin in oligodendrocytes. Potential significance for multiple sclerosis. Mol. Cell Neurosci. 28, 390-401.

Massaro, A.R., 2002. The role of NCAM in remyelination. Neurol. Sci. 22, 429-435.

McCarthy, K.D., de Vellis, J., 1980. Preparation of separate astroglial and oligodendroglial cell cultures from rat cerebral tissue. J. Cell Biol. 85, 890-902.

McKinnon, R. D., Matsui, T., Ida, J.A., Dubois-Dalcq, M., Aaronson, S.A., 1990. FGF modulates th PDGF-driven pathway of oligodendrocyte development. Neuron 5, 603-614.

Milner, R., ffrench-Constant, C., 1994. A developmental analysis of oligodendroglial integrins in primary cells: changes in alpha v-associated beta subunits during differentiation. Development 120, 3497-3506.

Milner R, Frost, E., Nishimura, S., Delcommenne, M., Streuli, C., Pytela, R., ffrench-Constant, C., 1997. Expression of alpha v beta 3 and alpha v beta 8 integrins during oligodendrocyte precursor differentiation in the presence and absence of axons. Glia 21, 350-360.

Ng, T., Shima, D., Squire, A., Bastiaens, P.I.H., gschmeissner, S., Humphries, M.J., Parker, P.J., 1999. PKCα regulates β1 integrin-dependent cell motility through association and control of integrin traffic. EMBO J. 18, 3909-3923.

Norton, W.W., Cammer, W., 1984. Isolation and characterisation of myelin.In Myelin 2nd ed.(P. Morell ed., Plenum Press, New York), pp 147-180

Podulso, S.E., 1981. Oligodendroglia: bulk isolation and maintance as suspension cultures, Res. Meth. Neurochem. 5, 113-125 (ed. Marks, N., Rodknight, R. Plenum Press, New York)

Relvas, J.B., Setzu, A., Baron, W., Buttery, P.C., LaFlamme, S.E., Franklin, R.J., ffrench-Constant, C., 2001. Expression of dominant-negative and chimeric subunits reveals an essential rol for beta 1 integrin during myelination. Curr. Biol. 11, 1039-1043.

Richter-Landsberg, C., Heinrich, M., 1996. OLN-93: a new permanent oligodendroglia cell line derived from primary rat brain glial cultures. J. Neurosci. Res. 45, 161-173.

Sobel, R.A., Mitchell, M.E., 1989. Fibronectin in multiple sclerosis lesions. Am.J.Pathol. 135, 161-168.

Yong, V.W., Cheung, J.C.B., Uhm, J.H., Kim, S.U., 1991. Age-dependent decrease of process formation by cultured oligodendrocytes is augmented by protein kinase C stimulation. J. Neurosci. Res. 29, 87-99.